PERGAMON

International Journal of Solids and Structures 38 (2001) 4489–4505

INTERNATIONAL JOURNAL OF SOLIDS and STRUCTURES

www.elsevier.com/locate/ijsolstr

A study on determining true stress–strain curve for anisotropic materials with rectangular tensile bars

Z.L. Zhang [a,*], J. Ødegård [a], O.P. Søvik [b], C. Thaulow [a]

[a] *SINTEF Materials Technology, N-7465 Trondheim, Norway*
[b] *Hydro-Raufoss Automotive Research Centre, N-2831 Raufoss, Norway*

Received 30 April 1999; in revised form 30 April 2000

Abstract

Recently, a method has been proposed for determining material true stress–strain curve with rectangular tensile bars up to localized necking. In the proposed method, material true stress–strain curve can be directly calculated from the load versus thickness reduction (at the minimum cross-section) curve. The method was established based on the finite element (FE) analysis for isotropic materials. In this study, this method has been extended for materials with isotropic elastic properties but anisotropic plastic properties. Two cases, transverse anisotropy and planar anisotropy, have been considered. Hill's anisotropic material model implemented in ABAQUS was applied for the study. More than 30 three-dimensional FE analyses of rectangular specimens with different anisotropy value, hardening exponent and cross-section aspect ratio have been carried out. It is shown that the relation between thickness reduction and total area reduction of a given cross-section is influenced by material plastic anisotropy. It is, however, found that the anisotropic effect on the thickness–area reduction relation can be normalized by the width to thickness strain increment ratio r, and a modified thickness–area reduction relation is proposed and numerically and experimentally verified. One practical problem in tensile test is that it is difficult to predict the necking location. In this regard, a study on the sensitivity of initial notch geometry has been carried out. It is found that for a fixed initial notch radius, the percentage of error is approximately equal to the percentage of initial width reduction. The accuracy of using large initial width reduction can be improved by using large notch radius.

Keywords: True stress–strain curve; Anisotropic materials; Rectangular tensile specimens; Plastic forming

1. Introduction

The whole range true stress–strain curve of a material including material response in both the pre and post-diffuse necking stages is very important for metal forming analysis and for the analysis of ductile fracture. Material stress–strain curve before necking can be easily determined by using either round or rectangular tensile bars. There was, however, no method available for determining the whole range

* Corresponding author.
E-mail address: zhiliang.zhang@matek.sintef.no (Z.L. Zhang).

0020-7683/01/$ - see front matter
PII: S0020-7683(00)00302-4

stress–strain curve with rectangular tensile bars. The main challenge is to calculate the current minimum cross-section area of a tensile specimen. For anisotropic materials and also thin materials, it is very advantageous to use rectangular tensile bars. Recently, a method has been developed for determining true stress–strain curve by using rectangular tensile bars (Zhang et al., 1999). By measuring the thickness reduction at the minimum cross-section (Fig. 1) and the corresponding load, the true stress–strain curve can be easily calculated by the proposed method. The method was established based on the finite element (FE) analysis for isotropic materials. Many engineering alloys, however, display anisotropic plastic behaviour (Lademo, 1997a,b). In this study, the method has been extended to materials with isotropic elastic properties but anisotropic plastic properties. It is shown that the relation between thickness reduction and total area reduction of a given cross-section is influenced by materials plastic anisotropy – the width to thickness strain increment ratio, r. For r larger than 1, the previous isotropic relation underestimates the area reduction for a given thickness reduction, and vice versa. An attempt has been made to modify the proposed relation for anisotropic materials. The simple anisotropic material model, Hill's yield model implemented in ABAQUS, was used (abaqus, 1996; Hill, 1989). Two cases, transverse anisotropy and planar anisotropy have been considered. By carrying out a large number of three-dimensional finite element method (FEM) analyses, it is found that the anisotropic effect on thickness–area reduction relation can be normalized by the width to thickness strain ratio, r, and a modified thickness–area reduction relation for anisotropic materials is proposed.

One practical problem in the tensile test is that it is difficult to predict the necking location, and an initial notch imperfection is often used to trigger necking. In this regard, a study on the sensitivity of initial notch geometry has been carried out. It is found that for a fixed initial notch radius which is three times the initial width, the percentage of error is approximately equal to the percentage of initial width reduction. The accuracy of using large initial width reduction can be improved by using large notch radius.

In the following, the equation for calculating the minimum cross-section area reduction (at the diffuse necking region) based on the thickness reduction of a rectangular tensile specimen for isotropic materials is briefly repeated first. Then, the anisotropic material model, the effect of plastic anisotropy on the area reduction equation is presented, and a new equation is proposed. Finally, the results of sensitivity analysis of notch imperfection on the true stress–strain curve and verification of the proposed method by comparing with experimental results are reported. A summary of the findings in this investigation is given in Section 7. The validity of the proposed equation is also discussed.

2. Thickness–area reduction equation for isotropic materials

Recently, an extensive three-dimensional numerical study for isotropic materials has been carried out on the diffuse necking behaviour of tensile specimens with rectangular cross-section. An approximate relation between the area reduction of the minimum cross-section and the measured thickness reduction is established (Zhang et al., 1999). Fig. 1 shows typical initial and deformed minimum cross-section and contact points for measuring thickness reduction of a tensile specimen. It is shown that the area reduction can be separated into two parts: the area reduction due to proportional deformation calculated directly from the thickness reduction and the non-proportional area reduction due to shape change of the cross-section. The total area reduction deviates from the proportional part once a diffuse necking starts, just after the maximum load. Numerical results show that the area reduction is controlled by two factors: the initial aspect ratio of the cross-section and materials hardening ability. After normalization with the cross-section aspect ratio and the strain at the maximum load, which is an important representation of materials plastic hardening ability, it has been found that the area reduction versus thickness reduction curves for all the materials investigated collapsed into one. Based on this finding, an area reduction equation has been developed. The total area reduction ratio of the cross-section for isotropic materials can be written as

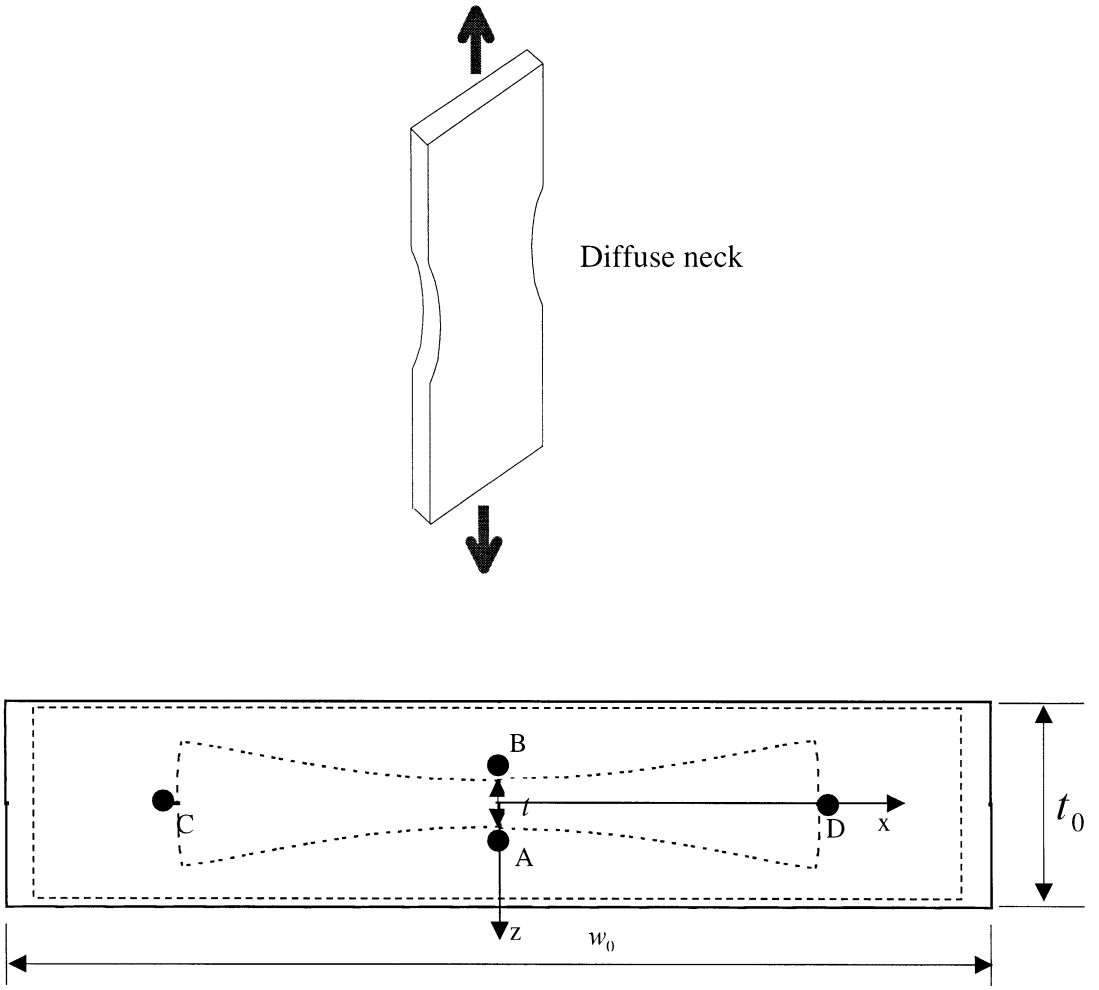

Fig. 1. Typical initial (—) and deformed (- - -) minimum cross-sections – proportional straining followed by non-proportional deformation: A and B are contact points for measuring thickness reduction, and C and D are points for measuring width reduction.

$$\frac{\Delta A}{A_0} = \left(\frac{\Delta A}{A_0}\right)_{\text{prop}} - f_s f_m f_t, \tag{1}$$

where the first term on the right-hand side denotes the area reduction due to proportional thickness reduction, and the second term denotes the area reduction due to shape change of the cross-section. Before the maximum load, the deformation of the cross-section is proportional and the cross-section does not change shape (Fig. 1). The second term comes into effect only when the necking starts, just after the maximum load is reached.

The proportional part in Eq. (1) can be easily written as

$$\left(\frac{\Delta A}{A_0}\right)_{\text{prop}} = 2\left(\frac{\Delta t}{t_0}\right) - \left(\frac{\Delta t}{t_0}\right)^2. \tag{2}$$

In Eq. (1), $f_s(S)$ is the function of cross-section aspect ratio, $S = w_0/t_0$, (Fig. 1) which has been found as (Zhang et al., 1999):

$$f_s(S) = 0.1686 + 0.6\ \ln(S). \tag{3}$$

The material hardening effect on the non-proportional area reduction is characterized by one material parameter – the thickness reduction ratio at the maximum load, $(\Delta t/t_0)_{P_{\max}}$. A linear equation has been obtained for the material hardening function, f_{m},

$$f_{\mathrm{m}}\left(\left(\frac{\Delta t}{t_0}\right)_{P_{\max}}\right) = 0.2845 - 0.956\left(\frac{\Delta t}{t_0}\right)_{P_{\max}}. \tag{4}$$

After the area reduction ratio has been normalized by the aspect ratio function, f_s, and the material hardening function, f_{m}, a geometry and material independent function is obtained. This function has been fitted by the following equation:

$$f_t(x) = c_0 + c_1 x + c_2 x^2 + c_3 x^3 + c_4 x^4, \tag{5}$$

where $x = \Delta t/t_0 - (\Delta t/t_0)_{P_{\max}}$ and the constants are

$$\begin{aligned} c_0 &= -0.03069,\\ c_1 &= 1.09016,\\ c_2 &= 11.1512,\\ c_3 &= -25.1,\\ c_4 &= 14.8718. \end{aligned} \tag{6}$$

Eq. (1) has been verified for materials with various hardening laws and for specimens with aspect ratio less than and equal to 8. Numerical verification has shown that Eq. (1) is very accurate (Zhang et al., 1999).

3. Anisotropic materials and anisotropic plastic model

Eq. (1) was developed for isotropic materials. Many extruded aluminium alloys, however, exhibit anisotropy in mechanical properties due to the crystallographic texture caused by the extrusion process. It has been observed that the anisotropy in elasticity is usually less significant compared with anisotropy in plasticity, and anisotropic plastic models must be used to describe the plastic behaviour of the alloys (Lademo, 1997a,b). Several anisotropic material models, including the Hill model, the Barlart model (Barlet and Lian, 1989; Barlet et al., 1997) and the model by Karafillis and Boyce (1993), have been recently reviewed by Lademo (Lademo, 1997a,b). It was concluded that none of the existing models with associated flow rule were able to completely describe the anisotropic flow properties observed in uniaxial tensile tests.

In this study, it is not intended to study how the anisotropic plastic flow behaviour can be described by an advanced anisotropic model. Rather, the purpose was to investigate how the shape change of the cross-section is influenced by the anisotropic deformation behaviour, i.e., to derive a relation between the area reduction and an anisotropic strain parameter (not the stress parameters which describe anisotropic plastic flow function).

In this study, a relative simple model, Hill's model implemented in ABAQUS was used. Hill's yield function is an extension of the conventional Mises yield function to allow anisotropic material behaviour. The function is written as

$$f(\sigma) = \sqrt{F(\sigma_y - \sigma_z)^2 + G(\sigma_z - \sigma_x)^2 + H(\sigma_x - \sigma_y)^2 + 2L\tau_{yz}^2 + 2M\tau_{zx}^2 + 2N\tau_{xy}^2}, \tag{7}$$

where F, G, H, L, M, and N are constants characteristic of the current state of anisotropy at different orientations. In ABAQUS, Hill's yield function equation (7) is defined from user input consisting of different ratios of yield stress in different directions with respect to a reference stress. In the FEM models used in this study, y-axis is the tensile axis, x represents the width direction of the cross-section and z is the thickness direction (Fig. 1). The yield stress in the y-axis has been taken as the reference yield stress. Therefore, the yield stress ratio in y-axis is always 1.0, $\alpha_y = \sigma_y/\sigma_y = 1.0$. The yield stress ratios in the x and z directions, α_x and α_z, have been changed to reflect different material anisotropy. When the yield stress ratios have been defined, ABAQUS will calculate the anisotropy parameters according to the following equations:

$$\begin{aligned} F &= \frac{1}{2}\left(1+\frac{1}{\alpha_z^2}-\frac{1}{\alpha_x^2}\right),\\ G &= \frac{1}{2}\left(\frac{1}{\alpha_z^2}+\frac{1}{\alpha_x^2}-1\right),\\ H &= \frac{1}{2}\left(1+\frac{1}{\alpha_x^2}-\frac{1}{\alpha_z^2}\right),\\ L &= \frac{1.5}{\alpha_{yz}^2}, \qquad M = \frac{1.5}{\alpha_{xz}^2}, \qquad N = \frac{1.5}{\alpha_{xy}^2}. \end{aligned} \tag{8}$$

Once the anisotropy stress parameters have been calculated, the anisotropic strain parameter, width to thickness strain increment ratio can be obtained

$$r = \frac{\mathrm{d}\varepsilon_x}{\mathrm{d}\varepsilon_z} = \frac{H}{F}. \tag{9}$$

Both transverse anisotropy, $\alpha_x = \alpha_y = 1$, $\alpha_z \neq 1$, and a special case of planar anisotropy, $\alpha_z = \alpha_y = 1$, $\alpha_x \neq 1$ have been considered. The conclusions drawn have been verified to the general anisotropy case, $\alpha_x \neq \alpha_z \neq \alpha_y$. In all the analyses, the shear components of the anisotropy constants have been taken to be zero. In total, more than 30 analyses of tensile specimens with varying anisotropy, hardening exponent and aspect ratio have been performed.

4. Thickness–area reduction for anisotropic materials

4.1. "Isotropized" thickness reduction

For isotropic materials, the thickness strain at maximum load is an important parameter for describing material's hardening ability. For anisotropic materials, the stress–thickness strain curves depend also on the plastic anisotropy. Fig. 2a shows the FE analysis results on the effect of plastic anisotropy on stress–thickness strain curves. The material hardening exponent in Fig. 2 is $n = 0.1$, and aspect ratio is 4. The same power-hardening law as (Zhang et al., 1999) was used, $\overline{\sigma} = \sigma_0(1 + \overline{\varepsilon}_\mathrm{p}/\varepsilon_0)^n$, where $\overline{\sigma}$ is the flow stress corresponding to the equivalent plastic strain $\overline{\varepsilon}_\mathrm{p}$, σ_0 is the yield stress, ε_0 is the yield strain $\varepsilon_0 = \sigma_0/E$, and E the Young's modulus. The r value varied from 0.14 to 3.57. The numerical procedure used in the present analyses are the same as used in (Zhang et al., 1999). It can be seen that the thickness strain at maximum load (necking strain) decreases with the increase of r value and thus indicates that the previous thickness–area reduction equation for isotropic materials cannot be directly applied to anisotropic materials. Fig. 2a shows that plastic anisotropy effect comes into play when the plastic deformation starts. However, in uniaxial tensile test, materials with different flow properties in width and thickness directions but same flow property in tensile direction should result exactly in the same total area reduction at a given tensile load. For isotropic materials, the true strain before necking can be written:

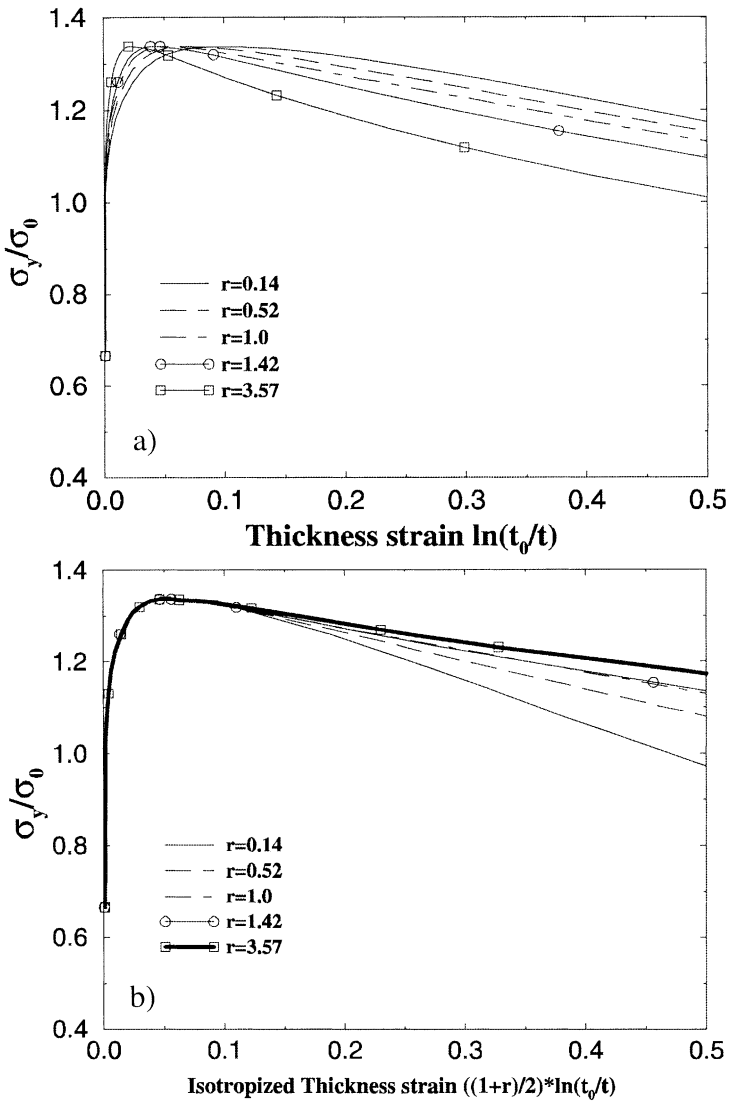

Fig. 2. (a) Examples on the effect of plastic anisotropy on stress–thickness strain curves for material with hardening exponent $n = 0.1$, and aspect ratio $S = 4$, and (b) stress versus isotropized thickness strain curves. σ_y is the gross stress.

$$\ln\left(\frac{A_0}{A}\right) = 2\varepsilon_t, \tag{10}$$

where, ε_t is the thickness average strain. For anisotropic materials the above equation becomes

$$\ln\left(\frac{A_0}{A}\right) = \varepsilon_t + \varepsilon_w = (1 + r)\varepsilon_t. \tag{11}$$

In order to study the effect of plastic anisotropy on the area versus thickness reduction curve, the thickness average strain can be "isotropized" from Eqs. (10) and (11)

$$\left(\frac{\Delta t}{t_0}\right)_I = \frac{1+r}{2}\left(\frac{\Delta t}{t_0}\right). \tag{12}$$

Fig. 2b shows the stress versus *isotropized* thickness strain curves. It can be seen that after isotropizing, the stress–thickness strain curves before necking become independent of the plastic anisotropy (necking occurs at the same thickness strain as the isotropic one); however, the curves after necking is still dependent on the plastic anisotropy. In the following, we will study the possibility to normalize the anisotropy effect.

4.2. The effect of anisotropy on the area reduction curve

By fixing material hardening parameter and the specimen aspect ratio, we now study the effect of plastic anisotropy by investigating the difference of area reduction between an anisotropy case and the corresponding isotropy case:

$$\left(\frac{\Delta A}{A_0}\right)_{\text{Dif}} = \left(\frac{\Delta A}{A_0}\right)_{\text{Aniso}} - \left(\frac{\Delta A}{A_0}\right)_{\text{Iso}}. \tag{13}$$

Fig. 3 shows the anisotropy effect on the area reduction (Eq. (13)) versus net isotropized thickness reduction for the cases $r < 1.0$, both for planar anisotropy and transverse anisotropy. In Eq. (13), the istropized thickness reduction (Eq. (12)) is used. Because of this, the influence of anisotropy on the area reduction curve starts only after the maximum load is reached. It can be observed that the area versus isotropized thickness reduction curves have similar pattern up to the range of 50% isotropized thickness reduction. For the cases $r < 1.0$, the anisotropy increases the area reduction at a given isotropized thickness reduction compared with isotropic material. In other words, the isotropic thickness–area reduction (Eq. (1)) would underestimate the total area reduction. For $r > 1.0$, the observation is opposite (Fig. 4). Fig. 3 shows that no matter whether it is planar anisotropy or transverse anisotropy, same r value yields nearly the same difference in area reduction.

A normalization procedure has been applied to Fig. 3 such that all the curves are normalized by its value at 50% of isotropized thickness reduction. The normalized curves are shown in Fig. 5. It is interesting to see

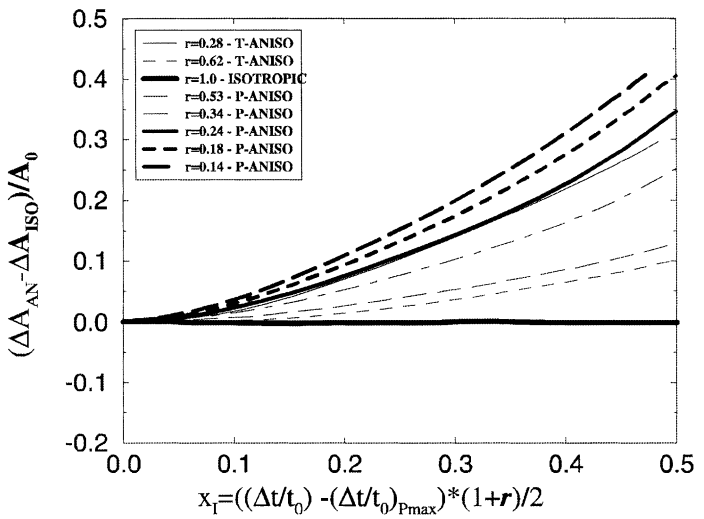

Fig. 3. The anisotropy effect on area reduction versus net isotropized thickness reduction curve for $r < 1.0$. In the legend, P stands for planar and T for transverse.

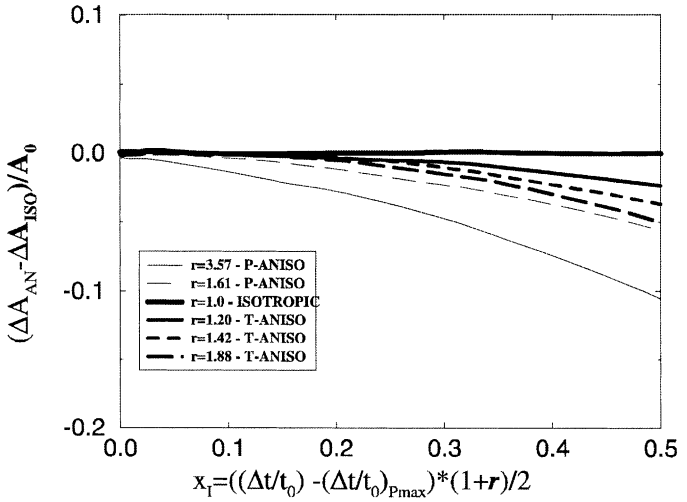

Fig. 4. The anisotropy effect on area reduction versus net isotropized thickness reduction curves for $r > 1.0$.

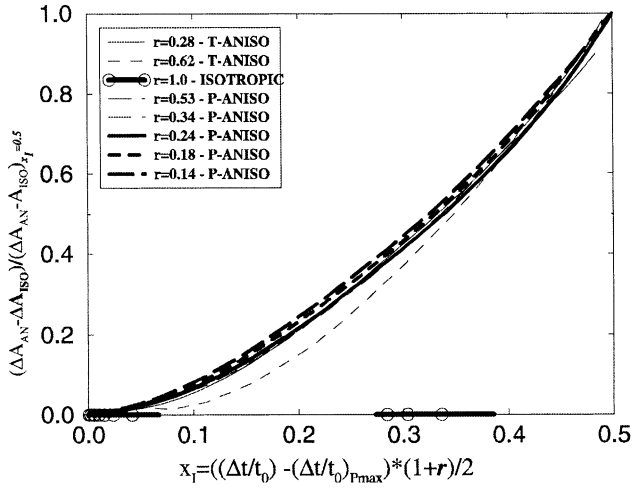

Fig. 5. Normalized area reduction versus thickness reduction curves for $r < 1.0$ (normalized form of Fig. 3).

that all the curves nearly collapse into one. This observation indicates that the effect of plastic anisotropy on area reduction can be normalized by a function of the parameter r. Similar observation has been seen with Fig. 4, and the normalized curves for Fig. 4 are nearly identical to the ones shown in Fig. 5. One typical curve has then been selected and fitted in Fig. 6 by the following equation:

$$f_I(x) = g_0 + g_1 x_I + g_2 x_I^2 + g_3 x_I^3, \tag{14}$$

where $f_I(x)$ is the y axis of Fig. 5, $x_I = 1 + r/2(\Delta t/t_0 - (\Delta t/t_0)_{P_{\max}})$ and

$$g_0 = -0.02156, \qquad g_1 = 0.79123, \qquad g_2 = 1.54188, \qquad g_3 = 1.91116. \tag{15}$$

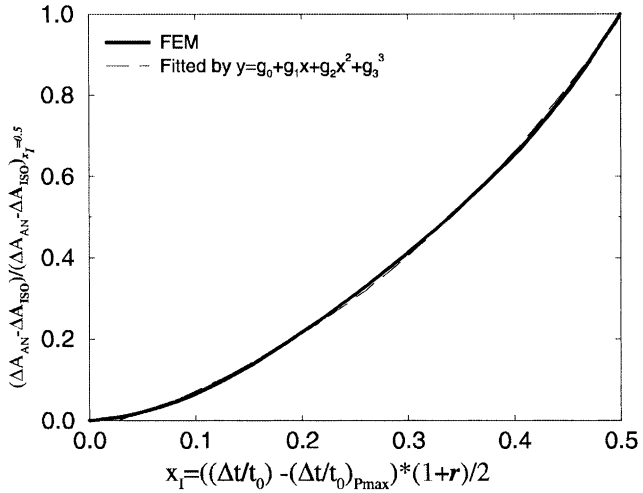

Fig. 6. Representative FE result and fitted solution for the unqiue anisotropy function-normalized area reduction versus isotropized net thickness reduction curve.

The quantities used for the normalization for the curves shown in Figs. 3 and 4 have been plotted against the corresponding r values in Fig. 7. Two approximate linear relations (for $r < 1.0$ and $r > 1.0$, respectively) can be seen. The curve shown in Fig. 7 has also been numerically fitted with the following equation:

$$f_r(r) = d_0 + d_1 r + d_2 r^2 + d_3 r^3 + d_4 r^4, \tag{16}$$

where $f_r(r)$ is the y axis in Fig. 7 and

$$d_0 = 0.62957, \qquad d_1 = -1.43536, \qquad d_2 = 1.16154, \qquad d_3 = -0.41161, \qquad d_5 = 0.051176. \tag{17}$$

Eq. (14), Fig. 6 represents the unique function for plastic anisotropy, which is independent of the value of plastic anisotropy parameter, while the effect of the absolute value of plastic anisotropy is considered in Eq. (16) (Fig. 7).

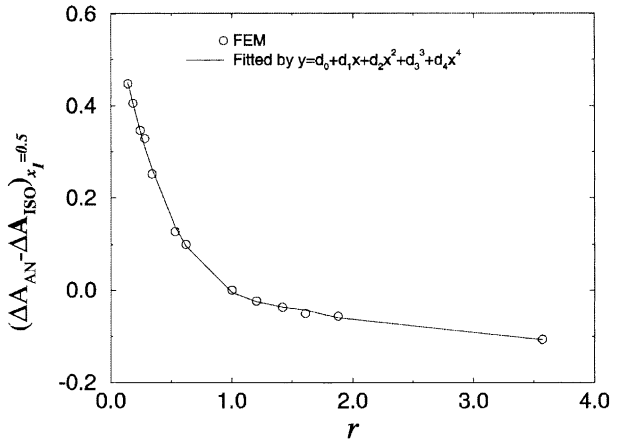

Fig. 7. The effect of anisotropy on the normalizing quantities.

4.3. New thickness–area reduction equation for anisotropic materials

Section 4.2 shows that the area reduction after diffuse necking caused by plastic anisotropy can be normalized by a function of the anisotropy strain parameter, r. The area reduction caused by plastic anisotropy belongs to material property and should be independent of the geometry characteristic (the aspect ratio function). By this reasoning and summarizing the results from Figs. 3–7, we get the following new area reduction equation for anisotropic materials:

$$\frac{\Delta A}{A_0} = r\left(\frac{\Delta t}{t_0}\right) - \frac{(1+r)^2}{4}\left(\frac{\Delta t}{t_0}\right)^2 - f_s(S)[f_t(x_I)f_{\mathrm{m}}(n_I) - f_I(x_I)f_r(r)], \tag{18}$$

where

$$\begin{aligned} x_I &= \left(\frac{1+r}{2}\right)\left[\left(\frac{\Delta t}{t_0}\right) - \left(\frac{\Delta t}{t_0}\right)_{P_{\max}}\right], \\ n_I &= \left(\frac{1+r}{2}\right)\left(\frac{\Delta t}{t_0}\right)_{P_{\max}}. \end{aligned} \tag{19}$$

For $r = 1.0$, Eq. (12) returns to the one for isotropic material. The same rule as for Eq. (1), the second term of Eq. (18) becomes active only after the maximum load has passed, i.e., when the deformation of the cross-section becomes non-proportional. In general, the area reduction equation for anisotropic material has the following form:

$$\frac{\Delta A}{A_0} = f\left(\frac{\Delta t}{t_0}, S, \left(\frac{\Delta t}{t_0}\right)_{P_{\max}}, r\right). \tag{20}$$

5. Numerical and experimental verifications

5.1. Numerical verifications

Eq. (18) has been numerically verified for tensile specimens with different aspect ratios and material hardening exponents. The comparison is shown in Figs. 7–11, where S is the section aspect ratio, n, the hardening exponent, and r, the width thickness strain ratio.

Figs. 8 and 10 shows that for $r < 1$ and both low and strong plastic hardening, the calculated true stress–strain curves from the procedure for isotropic materials (Eq. (1)) will cross with the "real" true stress–strain curve from FE analysis. However, the calculated curves according to the new procedure for anisotropic materials agree very well with the real curves, with less than 2% of error at 100% true strain. The general observation is that when $1.0 > r > 0.5$, the error by using the isotropic procedure for anisotropic materials is not significant.

The aspect ratio and material hardening in Figs. 9 and 11 are very different. It can be observed that the procedure for isotropic materials will result in significant error for the cases with $r > 1$. For low hardening material, a maximum point in the true stress–strain curve can be found if the procedure for isotropic material is used. Figs. 9 and 11 clearly show that the new procedure for anisotropic materials gives very satisfactory results. They also indicate that it is very important to consider the effect of plastic anisotropy on material true stress–strain behaviour in tensile tests, especially for the materials with $r > 1$.

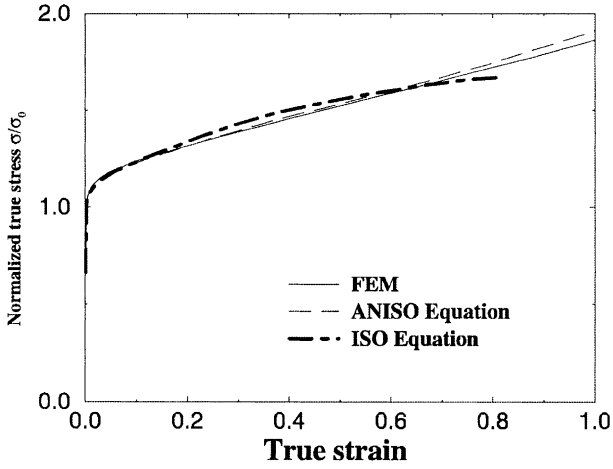

Fig. 8. Comparison of the prediction using isotropic and anisotropic equations with the FE results for $S = 5$, $n = 0.05$, $r = 0.42$.

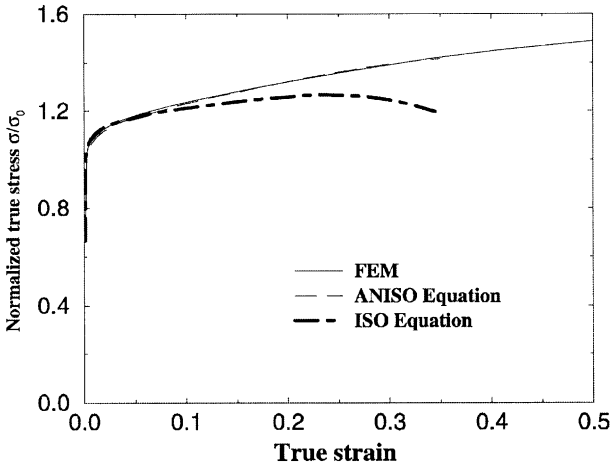

Fig. 9. Comparison of the prediction using isotropic and anisotropic equations with the FE results for $S = 5$, $n = 0.05$, $r = 2.38$.

5.2. Experimental verifications

An experimental programme has been carried out in (Zhang et al., 2000) to verify the proposed procedure. Thirty three tensile specimens with rectangular cross-section, including three aluminium alloys and one steel, have been tested. The cross-section aspect ratio varied from 2 to 4. The nominal plate thickness is 2.5 mm. Fig. 12 shows the profile of the cross-section for a 6060.35 T5 aluminium alloy with aspect ratio 2 and $r = 0.66$, measured from interrupted test specimen together with one from FEM analysis. This comparison shows that the cross-section of the tensile specimens for this aluminium alloy was well simulated by the FEM analysis.

Fig. 13a compares the true stress–strain curves for an aluminium 7108.70 T6 alloy determined by using the procedure for anisotropic materials from rectangular tensile specimens with aspect ratios, 2 and 4. The

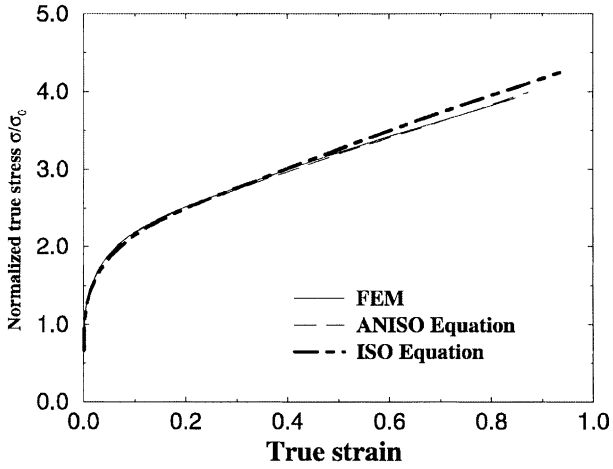

Fig. 10. Comparison of the prediction using isotropic and anisotropic equations with the FE results for $S = 5$, $n = 0.2$, $r = 0.7$.

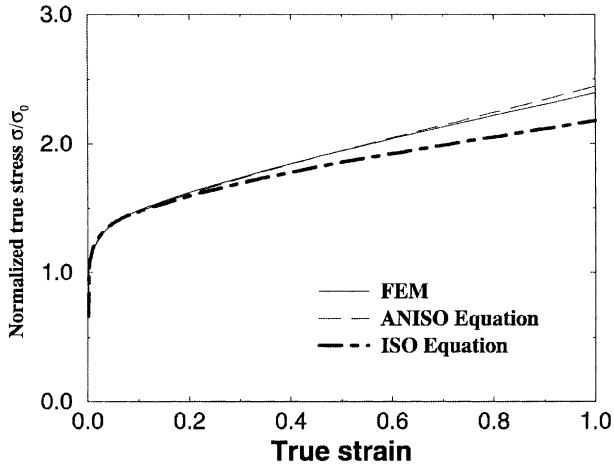

Fig. 11. Comparison of the prediction using isotropic and anisotropic equations with the FE results for $S = 2$, $n = 0.1$, $r = 1.42$.

number in the legend is the total test number in the verification programme. In total, nine tests were carried out for this alloy. We can observe that the results are independent of the cross-section aspect ratio. The scatter band is very small, less than 10 MPa.

The true stress–strain curve obtained from rectangular tensile specimens based on the procedure for anisotropic materials has been compared with the one obtained from conventional round tensile specimen with a diameter 4 mm (Fig. 13b) for the 71089.70 T6 alloy. The curve obtained according to the procedure for isotropic materials is also shown in the figure. There is a large difference between the curves obtained from the procedure for isotropic materials and anisotropic materials. The curve from the procedure for anisotropic materials is slightly lower than, but very close to the curve from the round specimens.

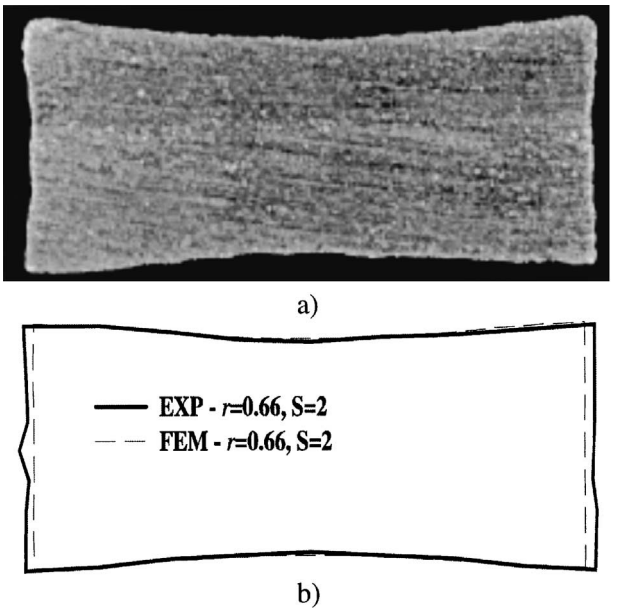

Fig. 12. (a) Deformed profile of a test specimen with cross-section aspect ratio 2 and (b) comparison of the test result and the predictions.

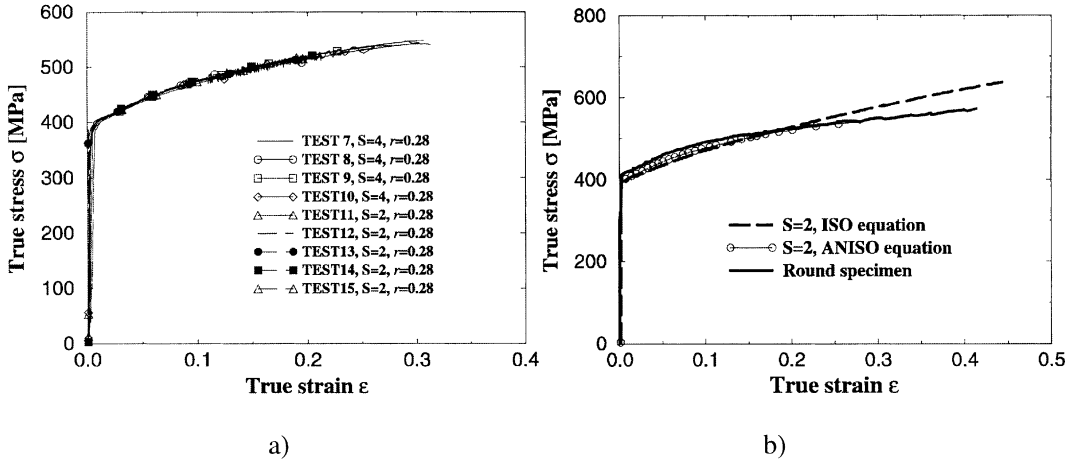

Fig. 13. (a) The true stress–strain curves determined from rectangular tensile specimens with two different aspect ratios, for the aluminium 7108.70 T6 alloy, and (b) comparison of the true stress–strain curve from rectangular and round specimens. "ISO" means the procedure for isotropic materials, and "ANISO" for anisotropic materials.

6. Effect of initial imperfection on the true stress–strain curve

One practical difficulty using Eq. (18) is that the location of final necking is difficult to predict for smooth tensile specimens. For practical purpose, it is advantageous to introduce some initial imperfection (Fig. 14), for example, an initial notch in the width direction shown in Fig. 12 so that the location of necking can be

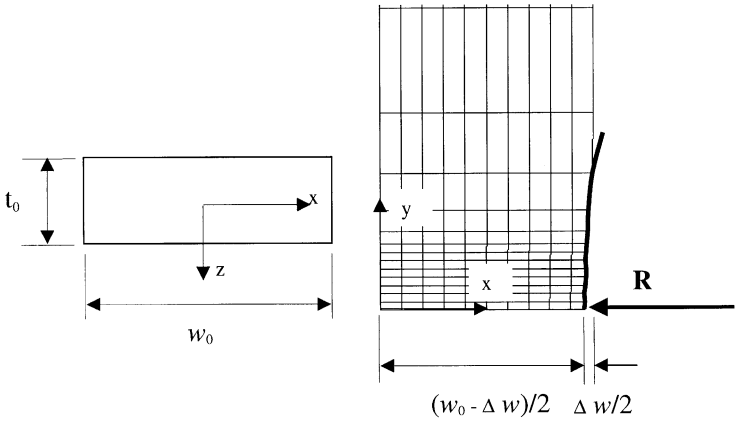

Fig. 14. Initial imperfection in the width direction.

predetermined. It is therefore important to study how the accuracy of the true stress–strain curve is influenced by the severity of the initial imperfection. Two parameters of the initial imperfection, the extent of the width reduction, $\Delta w/w_0$ and the notch radius, R, have been investigated. The aspect ratio of the tensile specimen was kept constant at 4, and only isotropic material with hardening exponent $n = 0.1$ has been considered. Totally, about 15 analyses have been carried out.

6.1. The effect of width reduction ratio, $\Delta w/w_0$

The range of the width reduction ratio, $\Delta w/w_0$ from 0.2% to 4% have been studied. Fig. 15 shows the in-plane meshes for the models with different $\Delta w/w_0$. The basic mesh pattern is exactly the same as the one used in (Zhang et al., 1999). Fig. 16 shows the effect of the width reduction ratio, $\Delta w/w_0$ for a given notch radius 30 mm which is three times the initial width, on the true stress–strain curves. It can be observed that the effect of width reduction ratio on the stress–strain curve was constant throughout the entire true strain range (curves with different imperfection do not cross each other). In general, specimen with initial imperfection will overestimate the true stress, and high width reduction $\Delta w/w_0$ results in higher true stress, indicating larger error. The effect of the $\Delta w/w_0$ on true stress at a true strain 1.5% is shown in Fig. 17. The error is calculated as $(\sigma_y^{\mathrm{FEM}} - \sigma_y^{\mathrm{Mat}})/\sigma_y^{\mathrm{Mat}}$, where σ_y^{Mat} is the material true (flow) stress inputted in the FE analyses. One rough conclusion that can be drawn from Fig. 17 is that the error in percentage is nearly equal to the percentage of initial width reduction.

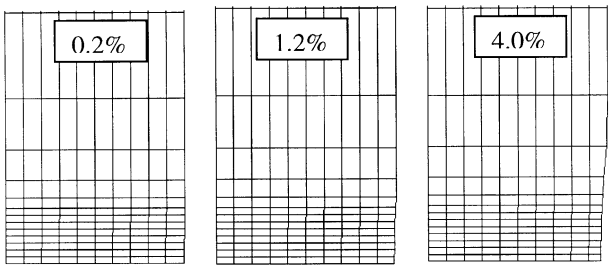

Fig. 15. Meshes in the x–y plane for different $\Delta w/w_0$ ratios: the aspect ratio is 4, and notch radius is three times the initial width.

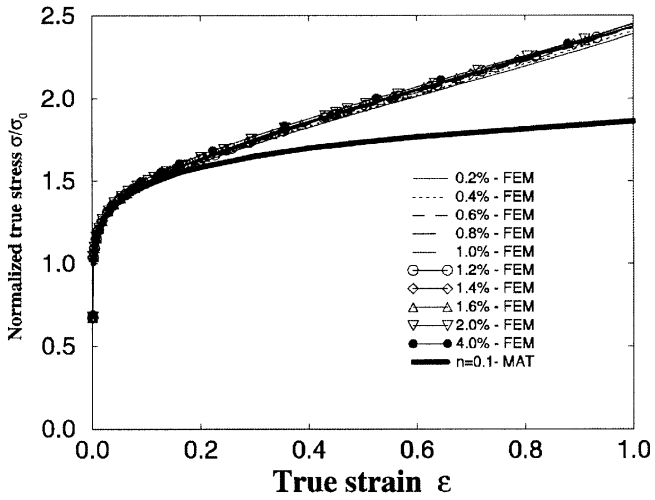

Fig. 16. The effect of $\Delta w/w_0$ on the global true stress–strain curves: the aspect ratio is 4, and notch radius is three times the initial width.

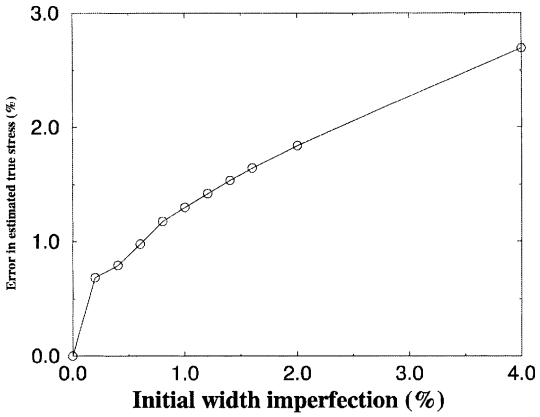

Fig. 17. Errors in calculated true stress versus initial width imperfection $\Delta w/w_0$: the notch radius is three times the initial width.

6.2. The effect of initial notch radius

For the model with width reduction ratio, $\Delta w/w_0 = 4\%$, the effect of notch radius on the accuracy has been investigated. Fig. 18 shows the in-plane meshes used in the study. Three notch radii, $R = 3w_0, 6w_0$ and $9w_0$ have been considered. The effect of notch radius on the true stress at a true strain 1.5% is shown in Table 1. It can be seen that for a given width reduction, the accuracy is improved by using larger notch radius, i.e., the error introduced by large width reduction is reduced by large notch radius. The error for an initial width reduction ratio 4% can be reduced 40% when the notch radius increases from $3w_0$ to $9w_0$. The degree of error for the case with 4% initial width reduction and $9w_0$ notch radius is approximately equal to the case with 1.2% initial width reduction and $3w_0$ notch radius. From these results, we can conclude that larger notch radius is generally preferred when a large imperfection is used.

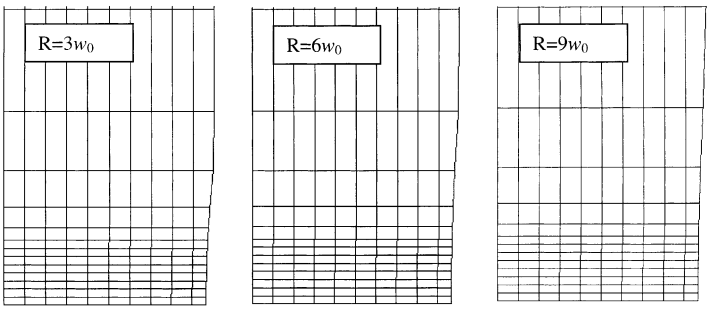

Fig. 18. Meshes used for the study of notch radius effect: width reduction ratio is 4%.

Table 1
Error versus initial notch radius

Notch radius	Error (%)
Infinite	0
$9w_0$	1.7
$6w_0$	2.1
$3w_0$	2.7

7. Summary

In order to determine the whole range true stress–strain curve, it is necessary to measure thickness reduction of the minimum cross-section of a tensile specimen. It is a common practice to apply an initial imperfection to the specimen so that the diffuse necking location can be predetermined. In this study, a sensitivity analysis of initial imperfection in the width direction of a rectangular cross-section tensile specimen on the true stress–strain curve has been carried out. It has been found that for a fixed notch radius $3w_0$, the percentage of error is approximately equal to the percentage of initial width reduction. The error can be reduced by applying a larger initial notch radius.

It has been found that the thickness–area reduction relation is influenced by the width to thickness strain ratio, r. For $r > 1$, the isotropic equation underestimates the thickness–area relation, and for $r < 1$, it is opposite. Numerical results have shown that the effect of anisotropy on the thickness–area reduction can be characterized as a function of r. Based on the FEM results, a new equation for calculating the total area reduction from the thickness reduction for anisotropic material has been proposed. The equations return to the isotropic equation for $r = 1.0$. The proposed equation has been numerically and experimentally verified for specimens with different aspect ratios, hardening exponent and r value. Very good accuracy is observed. Numerical verification has shown that it is very important to apply the new procedure for anisotropic materials, especially for materials with $r > 1$. Experimental verifications show that the procedure give very consistent results.

In this study, only yield strength anisotropy was considered. The elastic properties and hardening ability of the material were assumed to be isotropic. Anisotropy may exist in all the three aspects in semi-finished aluminium products; however, the elastic anisotropy effect may not be significant. Recent numerical results by Beaudoin et al. (1996) show that the yield surface shape was not drastically changed by the texture evolution, and it was reasonable to assume isotropic hardening.

Although a relatively simple yield function, Hill's model has been used. Hill's model may not be the best anisotropic material model for aluminium; however, as argued in Section 4, the specific material model may

not be crucial to the proposed thickness–area reduction equation because the thickness–area reduction was characterized by a deformation parameter, r, rather than a plastic flow stress parameter, for example, the α. This hypothesis should be verified both by tests and further numerical analysis.

The procedure to use the proposed method for determining true stress–strain curve for isotropic and anisotropic materials is summarized as follows: (1) Prepare the tensile specimens. The recommended aspect ratio is 4, and initial width imperfection is 1% and the notch radius is three times the initial width. (2) Measure the load, thickness reduction and width reduction according to the illustration shown in Fig. 1. (3) Determine the anisotropy parameter r according to Eq. (9) from the measured width–thickness strain relation. (4) Calculate the load versus area reduction curve with Eq. (18), and the true stress–strain curve. Finally, it should be noted that the resulting true stress–strain curve should be corrected by the Bridgman equation (Bridgman, 1952) before being used in FE analyses. The validity of Bridgman's correction to rectangular tensile specimens has been discussed by Zhang et al. (1999).

Acknowledgements

The financial support from the Norwegian Research Council (NFR) via the PROSMAT project is greatly acknowledged.

References

ABAQUS, 1996. User's Manual and Theory Manual, V5.5.

Beaudoin, A.J., Bryant, J.D., Dawson, P.R., Mika, D.P., 1996. Incorporating crystallographic texture in finite element simulations of sheet forming. In: Lee, J.K., Kinzel, G.L., Wagoner, R.H., (Eds.), Numisheet' 96, The Ohio State University, Columbus, USA. pp. 17–24.

Barlet, F., Lian, J., 1989. Plastic behaviour and stretch ability of sheet metals. Part I: a yield function for orthotropic sheets under plane stress conditions. Int. J. Plast. 5, 51–66.

Barlat, F., Maeda, Y., Chung, K., Yanagawa, M., Brem, J.C., Hayashida, Y., Lege, D.J., Murtha, S.J., Hattori, S., Becker, R.C., Makosey, S., 1997. Yield function development for aluminium alloy sheets. J. Mech. Phys. Solids 45, 1727–1763.

Bridgman, P.W., 1952. Studies in Large Plastic Flow and Fracture, McGraw Hill, New York.

Hill, R., 1989. The Mathematical Theory of Plasticity, Oxford University Press, New York.

Karafillis, A.P., Boyce, M.C., 1993. A general anisotropic yield criterion using bounds and a transformation weighting tensor. J. Mech. Phys. Solids 41, 1859–1886.

Lademo, O.-G., 1997a. Engineering models of elastoplasticity for aluminium alloys: an evaluation of yield criteria, flow rules and strain hardening rules. Report No. R-3.97, Department of Structural Engineering, The Norwegian University of Science and Technology (NTNU).

Lademo, O.-G., 1997b. State-of-the-art on elastoplastic constitutive models for aluminium alloys. Report No. R-30-97, Department of Structural Engineering, The Norwegian University of Science and Technology (NTNU).

Zhang, Z.L., Hauge, M., Ødegård, J., Thaulow, C., 1999. Determining material true stress–strain curves from tensile specimens with rectangular cross-section. Int. J. Solids Struct. 36, 3497–3516.

Zhang, Z.L., Ødegård, J., Søvik, O.P., 2000. Determining the true stress–strain curve for both isotropic and anisotropic materials with rectangular tensile bars: Methods and verifications, Computational Material Science, accepted.